Laser Photoacoustic Detection Allows in Planta Detection of Nitric Oxide in Tobacco following Challenge with Avirulent and Virulent *Pseudomonas syringae* Pathovars[1]

Luis A.J. Mur*, I. Edi Santosa, Lucas J.J. Laarhoven, Nicholas J. Holton, Frans J.M. Harren, and Aileen R. Smith

Institute of Biological Sciences, University of Wales, Aberystwyth, SY23 3DA, Wales, United Kingdom (L.A.J.M., N.J.H., A.R.S.); and Life Science Trace Gas Exchange Facility, Department of Molecular and Laser Physics, Catholic University of Nijmegen, 6525 ED Nijmegen, The Netherlands (I.E.S., L.J.J.L., F.J.M.H.)

We demonstrate the use of laser photoacoustic detection (LPAD) as a highly sensitive method to detect in planta nitric oxide ($^{\cdot}$NO) production from tobacco (*Nicotiana tabacum*). LPAD calibration against $^{\cdot}$NO gas demonstrated a linear relationship over 2 orders of magnitude with a detection threshold of <20 pmol h^{-1} (1 part per billion volume [ppbv]). The specificity of the photoacoustic signal for $^{\cdot}$NO when adding gas or the $^{\cdot}$NO donor, sodium nitroprusside, on injection into plant leaves, was demonstrated by its abolition with O_3 ($^{\cdot}NO + O_3 \rightarrow NO_2 + O_2$). The utility of the LPAD method was shown by examination of a nonhost hypersensitive response and a disease induced by *Pseudomonas syringae* (*P. s.*) pv *phaseolicola* and *P. s.* pv *tabaci* in tobacco. $^{\cdot}$NO was detected within 40 min of challenge with *P. s.* pv *phaseolicola*, some 5 h before the initiation of visible tissue collapse. The wildfire tobacco pathogen *P. s.* pv *tabaci* initiated $^{\cdot}$NO generation at 2 h postinfection. The use of $^{\cdot}$NO donors, the scavenger CPTIO ([4-carboxyphenyl]-4,5-dihydro-4,4,5,5-tetramethyl-3-oxide), and the mammalian nitric oxide synthase inhibitor L-NMMA (N^G-monomethyl-L-arginine) indicated that $^{\cdot}$NO influenced the kinetics of cell death and resistance to both avirulent and virulent bacteria in tobacco. These observations suggest that $^{\cdot}$NO is integral to the elicitation of cell death associated with these two bacterial pathogens in tobacco.

Nitric oxide ($^{\cdot}$NO), a well-characterized signal in mammalian systems (for review, see Wendehenne et al., 2001), is now being recognized as also influencing a variety of plant processes (for review, see Beligni and Lamattina, 2001). In particular, $^{\cdot}$NO plays an important role in plant defense responses, especially those associated with the hypersensitive response (HR) form of programmed cell death (for review, see Wendehenne et al., 2004). $^{\cdot}$NO generation has been observed following inoculation of avirulent (i.e. eliciting a HR) but not virulent bacterial strains into soybean (*Glycine max*; Delledonne et al., 1998) and Arabidopsis (*Arabidopsis thaliana*) suspension cultures (Clarke et al., 2000), as well as in tobacco (*Nicotiana tabacum*) epidermal peels treated with a necrotizing elicitor (Foissner et al., 2000). Recently, the expression of a bacterial $^{\cdot}$NO dioxygenase in transgenic plants to reduce $^{\cdot}$NO levels has demonstrated the role of $^{\cdot}$NO in the induction of cell death, the activation of the phenylpropanoid pathway, and in initiating the generation of reactive oxygen species (ROS; Zeier et al., 2004). Application of $^{\cdot}$NO elicited the formation of several features associated with mammalian apoptosis, including chromatin condensation, activation of caspase-like activity (Clarke et al., 2000; Pedroso et al., 2000), and loss of mitochondrial function that is associated with cytochrome c release (Saviani et al., 2002). $^{\cdot}$NO also has been shown to elicit the synthesis of the major defense signal salicylic acid (Dürner et al., 1998) and antagonize the effects of another, jasmonic acid (Orozco-Cardenas and Ryan, 2002).

In mammalian systems, $^{\cdot}$NO is synthesized by $^{\cdot}$NO synthase (NOS), which catalyzes the NADPH-dependent two-step oxidation of L-Arg to L-citrulline (Groves and Wang, 2000). By contrast, a range of sources of $^{\cdot}$NO have been proposed in plants. These include a novel inducible NOS (*AtNOS1*; Guo et al., 2003), nitrate reductases (Kaiser et al., 2002; Rockel et al., 2002; Sakihama et al., 2002), and nonenzymatic routes (Zweier et al., 1999; Bethke et al., 2004). In response to attack by phytopathogens, a NOS-like enzyme is perhaps the most likely source for $^{\cdot}$NO, as the mammalian NOS inhibitor L-NMMA (N^G-monomethyl-L-Arg) but not its inactive isomer D-NMMA (N^G-monomethyl-D-Arg) suppressed the HR with a resulting loss in disease resistance in Arabidopsis (Delledonne et al., 1998).

All these data notwithstanding, it remains the case that accurate measurements of in planta $^{\cdot}$NO generation

[1] This work was supported by the Biotechnology and Biological Sciences Research Council (grant no. P10096) and by the European Union (EU) Access to Research Infrastructure Action of the Improving Human Potential Programme. The Nijmegen facility was supported by the EU to act as a service unit for the measurement of trace gases. Scientists may apply to http://www.tracegasfac.science.ru.nl/index.html for use.

* Corresponding author; e-mail lum@aber.ac.uk; fax 44(0)1970–622350.

www.plantphysiol.org/cgi/doi/10.1104/pp.104.055772.

are still required (Beligni and Lamattina, 2001). For instance, the literature does not agree as to whether ·NO production is an early event during the prenecrotic phase of the HR (Delledonne et al., 1998; Clarke et al., 2000; Zeier et al., 2004) or a later phenomenon linked with the propagation of cell death (Zhang et al., 2003; Tada et al., 2004). Further, several effects of ·NO are concentration dependent, e.g. the ability of ·NO to break seed dormancy (Bethke et al., 2004) and the interaction with ROS/lipid-derived radicals (Beligni and Lamattina, 1999), the latter being an important feature of the elicitation of the HR (Levine et al., 1994; Chamnongpol et al., 1998) and gibberellin-induced programmed cell death in barley (*Hordeum vulgare*) aleurone layers (Fath et al., 2001). A comprehensive examination of ·NO and ROS interactions during the HR elicited by an avirulent strain of *Pseudomonas syringae* (*P. s.*) pv *glycinea* in soybean suspension cultures established that an interaction of ·NO and H_2O_2 was vital to the induction of cell death. Indeed, a stoichiometric imbalance in ·NO or H_2O_2 was proposed to reduce cell death (Delledonne et al., 2001). In programmed cell death linked to the barley aleurone and droughted wheat, ·NO appeared to be primarily suppressing cell death (García-Mata and Lamattina, 2001).

Many methods have been utilized to measure ·NO production. Most common are methods based on the oxidation of reduced hemoglobin (Delledonne et al., 1998) or the use of ·NO-specific fluorescent dyes, DAF-2DA (4,5-diaminofluorescein diacetate) and DAF-FM (4-amino-5-methylamino-2′,7′-difluorofluorescein; Foissner et al., 2000; Desikan et al., 2002). Dordas et al. (2003) exploited the fact that the ·NO unpaired π orbital allows its ready excitation by microwave and magnetic energy to measure ·NO using the specific spin trap Fe^{2+}-(dithiocarbamoyl)-*N*-methyl-D-glucamine)$_2$. Other measurement techniques sample directly from the gas phase as ·NO has a very low solubility (partition coefficient 0.04 = 4.6 mL/100 mL water at 20°C, 1 atm). A chemiluminescent approach, based on the reaction of ·NO gas with ozone ($\cdot NO + O_3 \rightarrow NO_2^* + O_2 \rightarrow NO_2$ + light), has been used to investigate the contribution of nitrate reductase to ·NO generation (Morot-Gaudry-Talarmain et al., 2002; Rockel et al., 2002). Very recently, two powerful methods based on mass spectrometry (MS) have been described. Bethke et al. (2004) described a continuous sampling method where ·NO was passed through a polyethylene membrane into the vacuum of a mass spectrometer. A similar technique was employed by Conrath et al. (2004) in the combined membrane inlet mass spectrometry (MIMS)/restriction capillary mass spectrometry (RIMS) approach, where ·NO can either diffuse from a culture through a membrane (MIMS) or from the gas phase through a thin restriction capillary (RIMS) directly into a benchtop mass spectrometer (Conrath et al., 2004). This approach allowed the sensitive detection of ·NO production from a variety of plant and fungal sources.

We have employed another direct-trace gas noninvasive, online sampling technique based on laser photoacoustic detection (LPAD; Bijnen et al., 1996; Harren et al., 2000). Although preliminary results have been published as conference proceedings (Mur et al., 2003), here we fully describe the high sensitivity (<20 pmol h^{-1}/<1 part per billion volume [ppbv]) and specificity of LPAD in the detection of ·NO. Further, we use LPAD to present a description of the kinetics of in planta production of ·NO in tobacco during a HR and disease development, revealing generation very early following pathogen challenge. Inhibitor studies suggested that ·NO contributes cell toward cell death and defense during both types of interaction.

RESULTS

Sensitive and Specific ·NO Detection Using LPAD

Preliminary studies have used LPAD in the detection of ·NO from plants (Leshem and Pinchasov, 2000; Mur et al., 2003), but the technique was not fully described and sensitivity and specificity of the approach was not determined. The experimental setup used in our LPAD experiments is depicted in Figure 1. An airflow was passed over the sample held in a sealed cuvette (Fig. 1, [1]) before being passed into the cold trap (Fig. 1, [4]) to remove excess water vapor, following which the sampled gas enters the photoacoustic chamber to be excited by chopped laser light (Fig. 1, [6]). Note that there is the possibility of measuring multiple samples by switching the gas flow to different cuvettes using valves (Fig. 1, [3]). Five laser lines were used to measure the ·NO concentration (Table I). Among them, the strongest ·NO line was at 1,900.0426 cm^{-1}. Due to the presence of water, one laser line (at 1,790.6576 cm^{-1}) served to determine the water concentration. The presence of other gases, such as ethylene and NO_2, was checked by the other lines. The photoacoustic principle is outlined in greater detail in ''Materials and Methods'' and elsewhere (Harren et al., 2000).

To determine the sensitivity of LPAD to ·NO, known concentrations were applied to the airflow in the photoacoustic chamber from a bottled ·NO source (Fig. 2A). The values obtained by LPAD revealed a near 1:1 predicted/measured relationship between approximately 28 pmol h^{-1} (1 ppbv) to approximately 4.5 nmol h^{-1} (200 ppbv) ·NO. ·NO readily forms NO_2 in the presence of O_3 ($\cdot NO + O_3 \rightarrow NO_2 + O_2$), and this was used to indicate the specificity of the photoacoustic signal. Addition of 0.2 L h^{-1} ·NO to a 1.3 L h^{-1} airflow established a photoacoustic signal and, following addition of 0.2 L h^{-1} O_3 to this mixture (with a concomitant reduction in air to maintain a constant gas flow), this was completely abolished (Fig. 2B). Removing O_3 from the gas flow resulted in the reestablishment of the ·NO photoacoustic signal.

Sodium nitroprusside (SNP; $Na_2[Fe(CN)_5(NO^+)]$) releases nitrosonium cations, which will readily nitrosylate

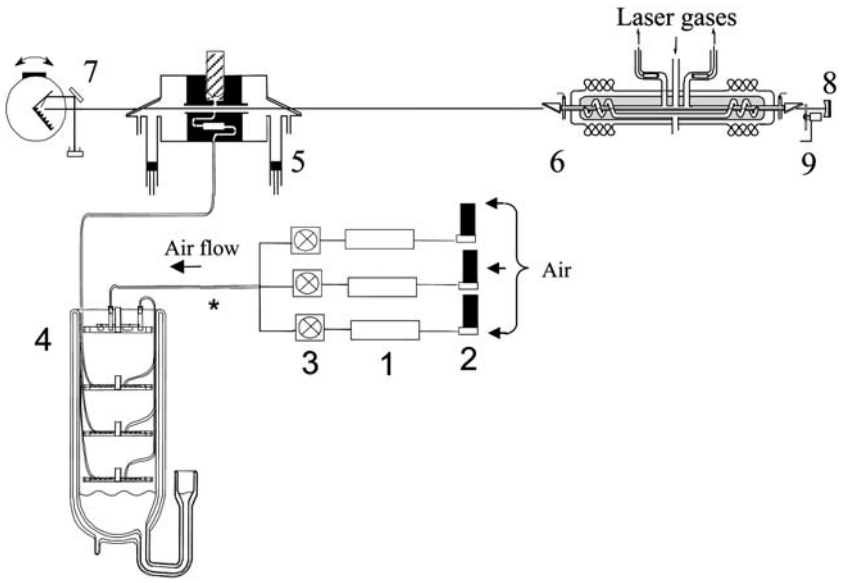

Figure 1. Experimental setup for CO LPAD of ·NO. Up to three samples (typically, a bacterially challenged leaf, a mock [water]-injected leaf, and an instrumental control [baseline]) were sealed in three glass cuvettes (1), which could be sampled by alternating electronic valves (3). Airflow (1.5 L h^{-1}) through the cuvettes was regulated by mass flow controllers (2). When not being sampled, the gas flow was vented from the cuvette to the atmosphere. Water vapor in the gas flow was removed using a Peltier cooling element (−5°C) and a cold trap (−80°C; 4), prior to passage into the photoacoustic cell (5). The photoacoustic cell was inserted into a laser cavity to improve laser power and, thus, detection sensitivity. This laser cavity consisted of a gas discharge tube (6), a rotatable grating (7; for laser line selection), and a 100% reflecting mirror (8). To generate a photoacoustic signal, the laser light was modulated by a chopper (9; modulation frequency 1,000 Hz). An additional water scrubber made of $CaCl_2$ (*) had no effect on the ·NO signal.

thiol groups and produce gaseous ·NO through homolysis of the S-N bond (Hughes, 1999). SNP is widely used as a nitrosylating agent in biological systems and has been used to validate ·NO detection by MS (Bethke et al., 2004). Various concentrations of SNP were injected into tobacco intercellular leaf spaces, and the emitted ·NO was monitored (Fig. 2C). At 1 h, ·NO production was proportional to added SNP, but at later time points, the higher concentrations of SNP appeared to yield lower levels of ·NO. This may indicate that, for some unknown reason, at higher concentrations the donor was more rapidly exhausted. To demonstrate that ·NO emissions were being measured from SNP, O_3 was added to the gas flow after passing through the cuvette (Fig. 2D). As in Figure 2B, application of O_3 completely abolished the ·NO photoacoustic signal, which was reacquired once O_3 was removed from the gas flow (Fig. 2D).

LPAD Reveals ·NO Emanation following Challenge with Both Avirulent and Virulent *P. syringae* Pathovars

Two approaches were used to measure ·NO emanation from tobacco following infiltration with bacterial cultures, as inoculated leaf areas require approximately 2 h to clear of injected liquid and it was thought that water-logged intracellular spaces could influence ·NO production or detection. For early measurements (0–2 h), leaves were explanted immediately after infiltration and sealed within the cuvette, while for longer time points (>2 h), leaves were kept on the plant for 2 h, allowing the infiltrated liquid to be mobilized out of the leaf and then removed for assay. With tobacco, the nonhost HR-eliciting strain *P. s.* pv *phaseolicola* and the virulent pathogen *P. s.* pv *tabaci* were utilized, which elicited distinctive phenotypes (Fig. 3A). The elicitation of HR by *P. s.* pv *phaseolicola* is dependent on a type III (hrp) secretion mechanism (Kenton et al., 1999) and, therefore, on the delivery of elicitory bacterial avirulence proteins into the plant cell (Collmer et al., 2000). Inoculation with *P. s.* pv *phaseolicola* resulted in a rapid increase in ·NO production after approximately 40 min (Fig. 3B), but, after 1 h, this was markedly reduced (Fig. 3C). The increased rates in ·NO production during the first hour averaged 17.01 (±0.81 SE; $n = 3$ experiments) nmol ·NO h^2 g^{-1} fresh weight (FW), which afterward were reduced to 3.08 (±0.47 SE) nmol ·NO h^2 g^{-1} FW. There was no evidence of ·NO production when inoculating with water (Fig. 3C) or extensive wounding using a wire brush (data not shown). Following challenge with *P. s.* pv *tabaci*, ·NO production was first detected after 2 h and increased to achieve approximately one-half the rate recorded with *P. s.* pv *phaseolicola* (Fig. 3, B and C).

The mammalian NOS inhibitor, L-NMMA, has been widely used in plant studies, so we sought to investigate its efficacy in suppressing ·NO levels in tobacco. Application of 1 mM L-NMMA, but not 1 mM D-NMMA, prior to the initiation of ·NO production by *P. s.* pv *phaseolicola* in controls suppressed ·NO

Table I. *The absorption coefficients for ·NO, water vapor, ethylene, and CO_2 at CO laser lines utilized in the analyses, together with their corresponding wavelengths*

The SD of the data (in parentheses) are in the units of the last digit.

Laser Lines $P(J'')_{v''}$	Wavelength	Absorption Coefficients		C_2H_4	CO_2
		·NO	Water		
	cm^{-1}	atm^{-1} cm^{-1}			
$P(7)_7$	1,933.4265	2.8 (2)	0.0079 (2)	0.303 (1)	0.0044 (1)
$P(10)_7$	1,921.8028	0.46 (5)	0.0215 (5)	0.70 (1)	0.0013 (1)
$P(9)_8$	1,900.0426	11 (1)	0.0014 (2)	0.568 (3)	0.000191 (4)
$P(7)_{10}$	1,856.4449	0.52 (5)	0.0059 (2)	0.8061 (5)	0.000013 (1)
$P(11)_{12}$	1,790.6576	0.094 (9)	0.40 (1)	0.0063 (3)	$<1.10^{-5}$

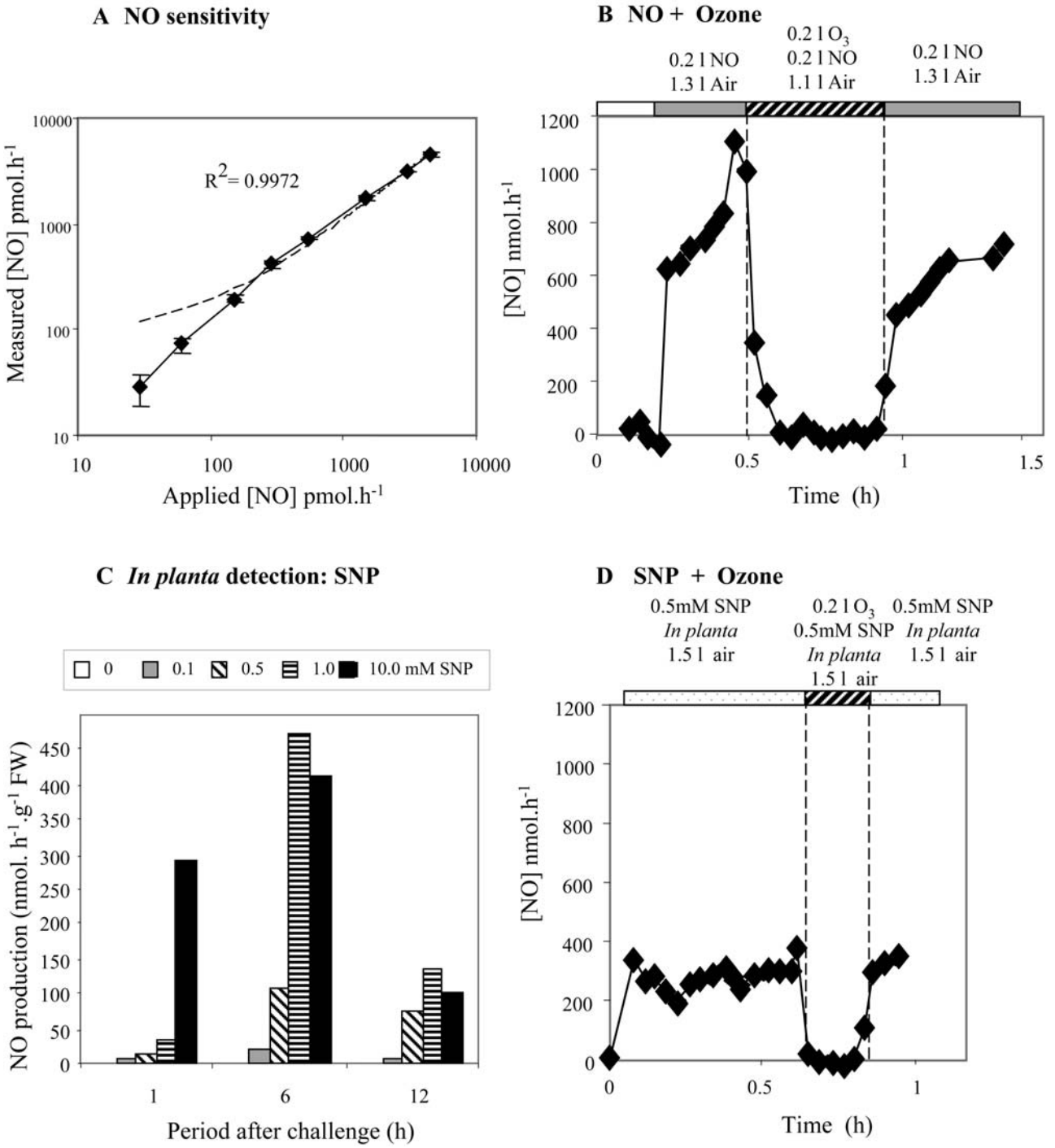

Figure 2. LAPD of ·NO. A, ·NO concentration measured with LAPD from ·NO mixtures in air. SD values are smaller than the symbols. A linear regression (note double log scale) through the data is added as a dashed line. B, Suppression of the ·NO photoacoustic signal with the application of O_3 ($\cdot NO + O_3 \rightarrow NO_2 + O_2$). ·NO was passed through the photoacoustic chamber at a rate of 0.3 L (from a bottled source) in 1.5 L h^{-1} air (gray rectangles). For an interval (diagonally hatched rectangle), the proportion of air was reduced to 1.1 L h^{-1} air to be replaced with 0.2 L h^{-1} O_3. C, ·NO production from tobacco leaves following injection with water (0, white bars) or 0.1 (gray bars), 0.5 (diagonally hatched bars), 1.0 (horizontally hatched bars), and 10 (black bars) mM of the $\cdot NO^+$/·NO donor SNP at 1, 6, and 12 h following injection. Results are given as nmol h^{-1} g^{-1} FW. D, ·NO levels detected following injection of 0.5 mM O_3 SNP (dotted rectangles), except during the period when 0.2 L O_3 was added to the gas flow after passage through the cuvette holding the leaf (diagonally hatched rectangle). Note that the results are given as nmol h^{-1} as the leaf weight was not recorded.

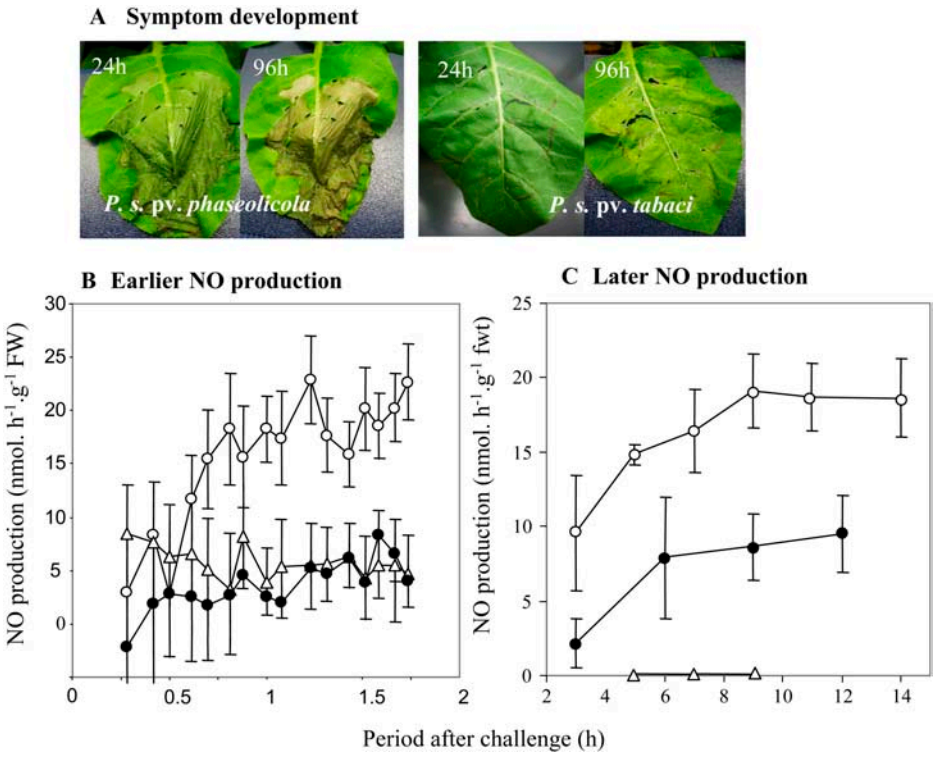

Figure 3. ·NO emanation in tobacco following challenge with avirulent and virulent *P. syringae* pathovars. A, *P. s.* pv *phaseolicola* and *P. s.* pv *tabaci* lesion phenotypes on tobacco at 24 and 96 h. Early (to 2 h; B) and later (>2 h; C) ·NO emanation from tobacco leaves following challenge with *P. s.* pv *phaseolicola* (white circles), *P. s.* pv *tabaci* (black circles), and water (white triangles). Results are given as mean ·NO production nmol h^{-1} g^{-1} FW ($n = 3$) ± SE.

production (Fig. 4). In case L-NMMA could be interfering with bacterial function, such as the delivery of elicitory protein(s), an additional experiment was undertaken in which inhibitors and ·NO scavengers were infiltrated into bacterially challenged areas after ·NO production had been initiated. Thus, ·NO production was measured in areas challenged with *P. s.* pv *phaseolicola* leaves at 3 h to establish the near steady-state production of ·NO (Fig. 3), after which the cuvette was opened and water, 1 mM L-NMMA, 1 mM D-NMMA, or 1 mM of the ·NO scavenger CPTIO (1*H*-imidazol-1-yloxy-2-[4-carboxyphenyl]-4,5-dihydro-4,4,5,5-tetramethyl-3-oxide) was injected. The cuvette was then resealed, and ·NO levels were determined after a further 0.5 h and compared to controls of *P. s.* pv *phaseolicola*-challenged leaves, where a second injection at 3 h had not been carried out. The results presented in Table II show that injection with water or D-NMMA did not significantly affect ·NO production, but both CPTIO and L-NMMA significantly reduced ·NO levels. Such data indicate that both CPTIO and L-NMMA are effective suppressors of in planta ·NO production.

Defense Responses to Avirulent and Virulent *P. syringae* Pathovars Are Influenced by ·NO in Tobacco

Investigations into the role of ·NO in tobacco interactions with avirulent and virulent *P. syringae* pathovars involved coinfiltrating bacterial suspensions with ·NO donors, NOS inhibitors, or ·NO scavengers. Preliminary experiments established that 0.5 mM SNP did not elicit plant cell death as assayed by electrolyte leakage during the first 24 h following infiltration. Further, when coinfiltrating tobacco leaves with 0.5 mM SNP and a *P. s.* pv *phaseolicola hrp*L mutant, which fails to elicit a HR (and therefore does not elicit many of the defense responses), bacterial viability was not directly affected at 24 h by the NO^+ donor (data not shown).

When inoculating with the avirulent *P. s.* pv *phaseolicola* strain, we made similar observations to other workers using analogous pathogen systems (e.g. Delledonne et al., 1998), namely, that ·NO played a role in the elaboration of a HR. Coapplication of ·NO donors (0.5 mM each), SNP (Fig. 5A), *S*-nitrosoglutathione (GSNO), and spermine NONOate (NONO; data not shown) accelerated cell death, while with CPTIO and L-NMMA, but not its inactive isomer D-NMMA, the HR was delayed by at least 3 h (Fig. 5B). These changes in the kinetics of cell death correlated with either the decreased or the increased *P. s.* pv *phaseolicola* population numbers (Fig. 5, C and D).

With compatible interactions involving *P. s.* pv *tabaci*, a lesion-scoring scheme based on five different phenotypes was drawn up, ranging from no response (score 0) to spreading necrosis and chlorosis extending over the central vein (score 4; Fig. 6A). After 7 d, control infections with *P. s.* pv *tabaci* exhibited variable symptom development (Fig. 6B), although >80% of the lesions showed either limited or extensive spread of necrotic and chlorotic symptoms (scores 3 and 4, respectively; Fig. 6A). Coinfiltration with 0.5 mM GSNO, NONO, and, especially, SNP significantly

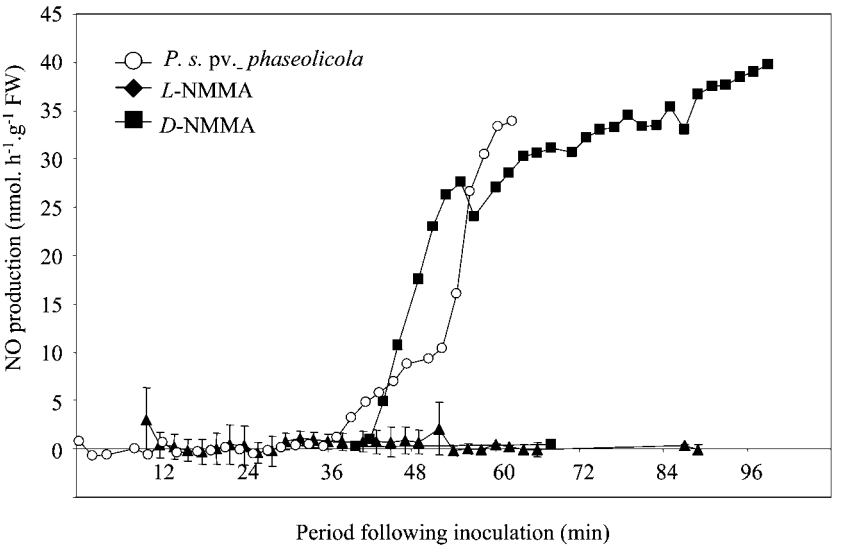

Figure 4. Suppression of ·NO production by the mammalian NOS inhibitor L-NMMA. ·NO production was estimated by LPAD in tobacco leaves immediately following infiltration with *P. s.* pv *phaseolicola* (white circles) and coinfiltration of *P. s.* pv *phaseolicola* with 1 mM L-NMMA (black diamonds, [$n = 3$] ± SE) or 1 mM D-NMMA (black squares). Data given for a single contemporaneous experiment that was later repeated to give similar results.

($P = <0.001$, χ^2) altered the distribution of lesion phenotype, with larger numbers exhibiting either localized necrosis with chlorosis (score 2) or only necrotic symptoms (score 1; Fig. 6B). Coapplication of CPTIO and, to a lesser extent, application of L-NMMA increased the numbers of lesions exhibiting extensive spreading necrosis/chlorosis (Fig. 6B; $P = <0.001$). The results of coinfiltration with D-NMMA gave a similar pattern to controls.

The magnitude of *P. s* pv *tabaci*-associated cell death could be augmented with the addition of SNP (Fig. 7A), although this was still delayed compared to those observed during a HR (Fig. 5A). Significantly, cell death associated with this compatible interaction could be suppressed with CPTIO and L-NMMA (Fig. 7B). Coapplication of SNP with *P. s.* pv *tabaci* reduced in planta bacterial growth (Fig. 7C), but CPTIO and L-NMMA appeared to have little effect on bacteria numbers within the infiltrated area until approximately 12 d postinfiltration (Fig. 7D, lesion). However, an examination of bacterial escape from the infiltrated areas suggested that application of CPTIO and L-NMMA, but not D-NMMA, facilitated bacterial escape from the lesion (Fig. 7D, surround).

DISCUSSION

The biological effects of ·NO are to a certain extent influenced by its concentration. For instance, in mammalian apoptosis, ·NO has antiapoptotic effects at low concentrations (10 nM to 1 μM), which were associated with *S*-nitrosation and inactivation of caspases (for review, see Brune et al., 1999), inhibition of mitochondrial permeability transition pore opening, and associated cytochrome c release (Brookes et al., 2000). At higher concentrations (>1 μM), there is an inhibition of mitochondrial ATP generation but promotion of mitochondrial permeability pore opening with concomitant cell death (Brookes et al., 1999, 2000). In plants, concentration-dependent effects of ·NO have been shown to influence the HR-type of cell death, probably by affecting the interaction with ROS (Delledonne et al., 2001; de Pinto et al., 2002). Thus, ·NO levels must be accurately determined in order to fully understand its action(s). Ideally, the assay method should be online, exhibit a high degree of sensitivity, linearity, and specificity, as well as allowing the determination of intra- or extracellular levels of ·NO from gas or liquid phases. Technically, the assay should be low cost, easy to carry out, and not dependent on highly specialized apparatus. In reality, all currently utilized methods fall short of this paradigm. Perhaps the most versatile is based on the formation of methemoglobin

Table II. *Inhibition of ·NO production during the HR by ·NO scavengers and NOS inhibitors*

Tobacco leaves ($n = 3$) were inoculated with bacterial suspensions of *P. s.* pv *phaseolicola* and placed in cuvettes, where ·NO levels were monitored by LAPD until steady production at 3 h (Fig. 3). At 3 h postchallenge, the cuvettes were opened and leaf areas inoculated with *P. s.* pv *phaseolicola* leaves were injected with water, 1 mM CPTIO, 1 mM L-NMMA, or 1 mM D-NMMA. The leaves were returned to the cuvettes, and ·NO levels were determined after a further 0.5 h. Hence, mean ($n = 3$ ± SE) ·NO production is given at 3.5 h postinoculation and compared to results obtained to control inoculations with *P. s.* pv *phaseolicola* ($n = 3$), which had not been injected the second time at 3 h. Differences between these means are indicated as either significant (***; $P = 0.001$) or not significant (^{NS}) following the *t test.*

Chemical	·NO Levels at 3.5 h following Challenge
	nmol $h^{-1}g^{-1}$ FW; $n = 3$ ± SE
P. s. pv *phaseolicola* inoculated at 3 h	33.9 (±0.6)
+water	34.5 (±2.2)^{NS}
+CPTIO	14.2 (±4.0)***
+L-NMMA	16.7 (±3.0)***
+D-NMMA	30.5 (±2.1)^{NS}

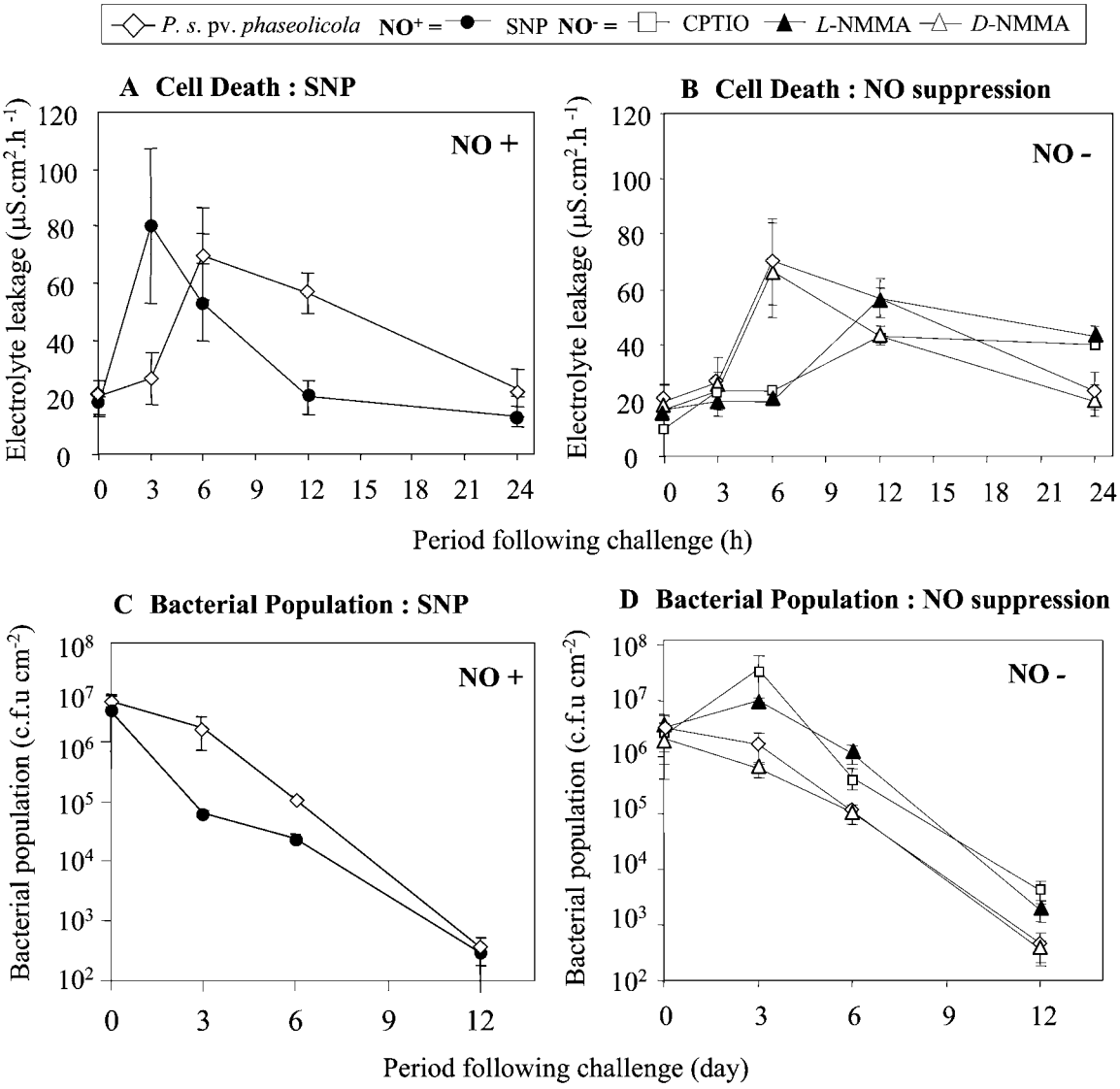

Figure 5. Modulation of ·NO-mediated events in the developing HR in tobacco as elicited by *P. s.* pv *phaseolicola*. A, The effects of coinfiltration of *P. s.* pv *phaseolicola* (white diamonds) with ·NO generators (NO^+, 0.5 mM SNP [black circles]); B, ·NO scavengers/inhibitors of NOS (NO^-, 1 mM of CPTIO [white squares], L-NMMA [black triangles], D-NMMA [white triangles]) on the conductivity of solution bathing explants (n = 6 treatment^{-1}). Results are given as mean conductivity change (μS cm^{-2} 3 h^{-1}) ± SE. Bacterial numbers were estimated in leaf areas (n = 6 treatment^{-1} time point^{-1}) coinfiltrated with *P. s.* pv *phaseolicola* with NO^+ (C) and NO^- (D) chemicals (see above). Results are given as mean cfu cm^{-2} ± SE.

from oxyhemoglobin, the relative levels of which are determined by measuring the A_{421} and A_{401}. Increases in methemoglobin can be calculated based on an extinction coefficient of 77 mM^{-1} cm^{-1} (Murphy and Noack, 1994). Therefore, this assay has few technical requirements and has a detection threshold of approximately 1 nmol (Archer, 1993), although it suffers from a sensitivity to ROS (Delledonne et al., 2001). DAF-2DA and DAF-FM dyes exhibit a high degree of specificity for ·NO (Kojima et al., 1998) and may be used to view ·NO generation, epidermal peels (Foissner et al., 2000), or in planta (Zhang et al., 2003). DAF dyes can be viewed by epifluorescence but preferably by confocal laser-scanning microscopes, which are now possessed by many research institutions. However, DAF dyes do not readily lend themselves to online monitoring and may be preferentially taken up by certain organelles, and accurate quantification is particularly difficult (Foissner et al., 2000). In mammalian systems, ·NO electrodes have been frequently used. These rely on the electrochemical oxidation of ·NO to generate an electric current and tend to be based on a modified oxygen (Clarke) electrode (Shibuki, 1990) or a porphyrinic semiconductor (Malinski et al., 1993). These ·NO electrodes have fast response times (sometimes less than 1 s) and specific sensitivities down to nanomolar levels (Leone et al., 1995) or lower (Archer, 1993). However, ·NO electrodes

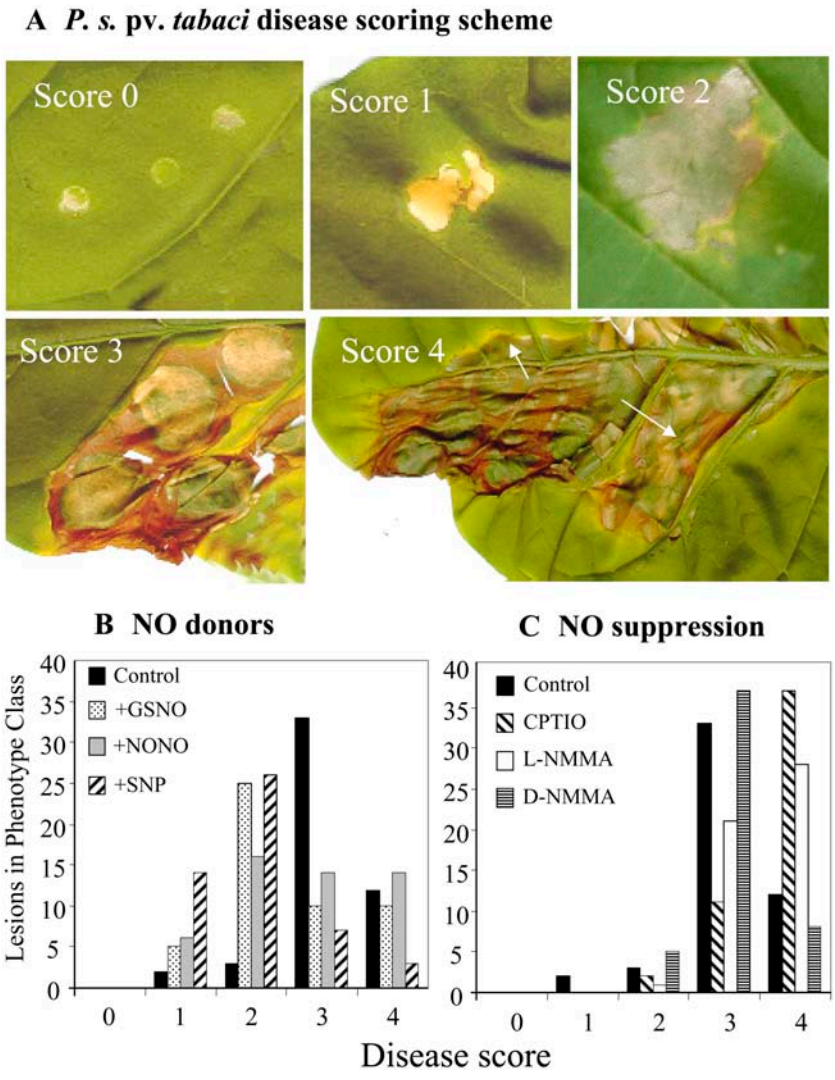

Figure 6. ·NO affects wildfire symptom development following inoculation of tobacco cv Samsun NN with of *P. s.* pv *tabaci*. A, Classification of *P. s.* pv *tabaci* lesion phenotypes at 7 d following infection. Score 0, No visible response; score 1, necrosis confined to the infection point, no chlorosis; score 2, confined necrosis with chlorosis; score 3, spreading necrosis with chlorosis; and score 4, extensive spreading necrosis and chlorosis. B, Disease scores of 50 lesions forming on control (black bars) and treated leaves coinfiltrated with bacteria and ·NO generators (NO^+, 0.5 mM each of GSNO [dotted bars], NONO [gray bars], and SNP [diagonally hatched bars]). C, ·NO suppressors (NO^-, 1 mM each of CPTIO [diagonally hatched bars], L-NMMA [white bars], and D-NMMA [horizontally hatched bars]) were noted at 7 d postinfiltration. This experiment was repeated and yielded similar data.

have only been used infrequently in plant systems, e.g. with unicellular green algae (Sakihama et al., 2002) or during high-level ROS generation (Delledonne et al., 2001). This limited use may be due to the difficulty of using ·NO electrodes in planta, although Leshem et al. (1998) measured ·NO in fruit by simply pushing the probe through the surface layers.

Other approaches to assay in planta ·NO production rely on special equipment, e.g. electron paramagnetic resonance (EPR) and MS-based techniques. In EPR, the unpaired ·NO electron is spin-trapped by nitrosocompounds or reduced hemoglobin to form a stable adduct. EPR exhibits a detection threshold of approximately 1 nmol (Archer, 1993), but it does not easily allow continuous ·NO detection in planta. By contrast, MIMS/RIMS represents a highly versatile approach by allowing online sensitive ·NO (approximately 1 nmol) and other gas detection from gaseous and liquid phases (Conrath et al., 2004). Another MS approach, where gaseous ·NO was measured after passage through a gas-permeable membrane, detected concentrations of approximately 1 μM (Bethke et al., 2004). A chemiluminescent assay for ·NO in the gaseous phase exhibits even greater sensitivity, with a detection threshold of approximately 20 pmol (Archer, 1993). The attraction of online assays of ·NO levels leads us to investigate an alternative approach to measure ·NO levels in the gaseous phase based on LPAD. Preliminary measures of ·NO from plants have been made with LPAD and sensitivities down to parts per trillion volume (pptv) have been claimed (Leshem and Pinchasov, 2000). Nevertheless, direct sampling of ·NO from the gaseous phase may underestimate concentrations within plant tissues, as it relies on the poor solubility of ·NO in aqueous solutions and cannot assess ·NO reduction (to form the nitroxyl anion, NO^-) or oxidation (to form the nitrosonium cation, NO^+), both of which have biologically relevant actions in, for instance, the formation of *S*-nitrosothiols (Hughes, 1999). As regards the latter point, it should be noted that all current assay methods target particular forms of ·NO, e.g. DAF-2DA/FM stains target NO^+ (Kojima et al., 1998).

Our estimations of the sensitivity of the photoacoustic technique to ·NO indicated that levels of

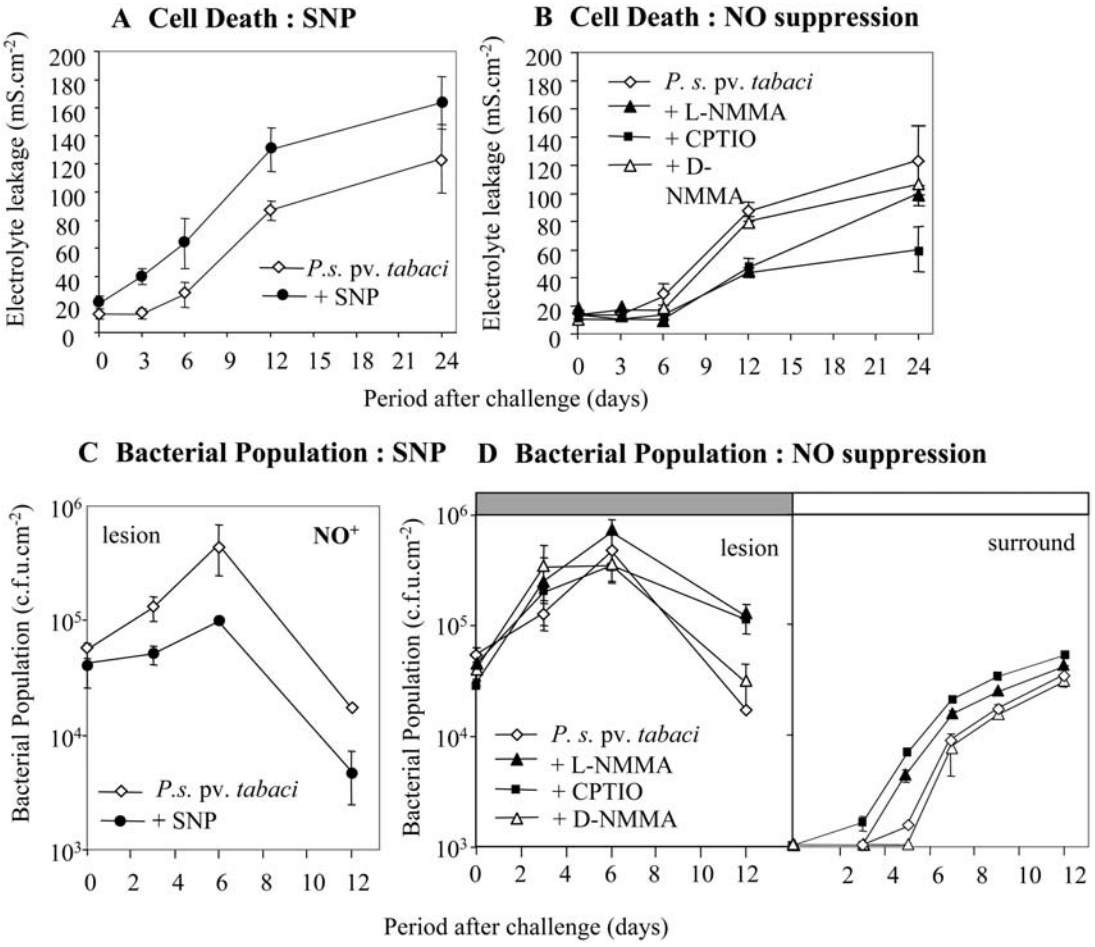

Figure 7. ·NO modulates compatible interactions between *P. s.* pv *tabaci* and tobacco cv Samsun NN. Changes in the conductivity of the solution bathing tobacco explants infiltrated with *P. s.* pv *tabaci* (white diamonds) and coinfiltrated with 0.5 mM SNP (black circles; A) and 1 mM each of CPTIO (black squares), L-NMMA (black triangles), and D-NMMA (white triangles; B; $n = 6$ treatment^{-1}). Results are given as mean conductivity (μS cm^{-2}) ± SE. Bacterial numbers were estimated in leaves within areas ($n = 6$) coinfiltrated (lesion) with *P. s.* pv *tabaci* (white diamonds) and with 0.5 mM SNP (NO^+; C) and 1 mM each of CPTIO (black squares), L-NMMA (black triangles), and D-NMMA (white triangles; D), within the lesion and also bacterial escape into surrounding tissue (surround). Results are given as mean cfu cm^{-2} ± SE.

1.3 ppbv (approximately 21.3 pmol h^{-1}) could be accurately measured, which were equivalent to thresholds for chemiluminescent detection (Archer, 1993) and greater than a 10-fold increased sensitivity compared to the RIMS approach (Conrath et al., 2004). Measurements of ·NO also exhibited a linear dynamic range over at least two orders of magnitude (Fig. 2A). Although the readings over five laser lines (Table I) were taken for each measurement, these were to assess possible contributions of other gases to the photoacoustic signal from ·NO laser line ($P(9)_8/1$, 900.0426 cm^{-1}). Hence, these readings for other gases were not optimized for their detection and cannot be considered the most valid means to assess their concentration. Therefore, for simultaneous detection of multiple gases, MIMS/RIMS (Conrath et al., 2004) and permeable-membrane MS (Bethke et al., 2004) represent attractive alternatives.

Validation of the ·NO signal was initially based on its physical characteristics (I.E. Santosa, L.J.J. Laarhoven, L.A.J. Mur, and F.J.M. Harren, unpublished data) but subsequently by its suppression using O_3 (Fig. 2B). Thus, we used O_3 to assess ·NO emissions from plant sources where many gases would be produced. Our in planta validation involved injections with SNP, an NO^+ donor, but which will produce ·NO gas via complex chemical reactions, e.g. homolysis of *S*-nitrosyl groups. LPAD indicated that, at least over the first hour following injection, an SNP concentration correlated with ·NO levels (Fig. 2C). Taken together, these data show that LPAD is a sensitive and specific method to assay ·NO production from in planta sources.

LPAD has previously been used for online measurements of ethylene (Cristescu et al., 2002; van den Bussche et al., 2003), acetaldehyde, and ethanol (Leprince et al., 2000; Boamfa et al., 2003) emanation in plants. We sought to demonstrate ·NO measurements in a plant system that has been extensively characterized by other workers, using standard scavenger/

inhibitor chemicals (e.g. CPTIO and L-NMMA). Thus, we determined ·NO production from pathogen-challenged tobacco leaves. The ·NO photoacoustic signal was suppressed by application of the NOS inhibitor L-NMMA (Fig. 4) and the ·NO scavenger CPTIO (Table II). Such data are supportive of a role for a plant NOS in pathogen-elicited ·NO production, but this does not rule out alternative sources of ·NO production. Antisense nitrate reductase plants have been used to suggest that this is a source of ·NO in light-stressed tobacco (Morot-Gaudry-Talarmain et al., 2002). In this study, only relatively minor increases in ·NO flux were detected (approximately 1 nmol g^{-1} h^{-1} FW) compared to those we measured following pathogenic challenge (>30 nmol g^{-1} h^{-1} FW), and this could indicate that different sources of ·NO production were being utilized.

Although our data confirm key elements of earlier work, in other ways they reveal some distinctive differences. During the nonhost HR in tobacco elicited by *P. s.* pv *phaseolicola*, a biphasic generation of ·NO (as reported by Delledonne et al. [1998] in soybean cultures and by Conrath et al. [2004] in tobacco cultures) was not seen. Instead, an early burst of ·NO production was noted, following which ·NO was produced at a constant rate. Clarke et al. (2000) also failed to observe a biphasic rise in ·NO in Arabidopsis cultures challenged with an avirulent strain of *P. s.* pv *maculicola* M6. Such contradictory observations could indicate that patterns of ·NO generation are interaction specific. To our knowledge, *P. s.* pv *phaseolicola* elicits an hrp-dependent (Kenton et al., 1999) HR in all varieties of tobacco and therefore must be considered an example of nonhost HR. The elicitation of such nonhost HR, as opposed to gene-for-gene (pathogen avirulence gene with host resistance gene)-mediated HR, is likely to be mediated by multiple interactions between host and pathogen (Mysore and Ryu, 2004). As this was likely also to be the case with the *P. s.* pv *maculicola* M6 strain (Rohmer et al., 2003), the lack of a biphasic ·NO burst in our two studies could be the net effect of overlapping elicitory events.

A consistent feature of our online assay with that of Conrath et al. (2004) is the early production of ·NO during the elicitation of a HR. This is contrary to the observations of Zhang et al. (2003) and Tada et al. (2004), who, using DAF-2DA dyes, failed to detect ·NO rises prior to cell death and therefore proposed that ·NO contributed to the elaboration of the HR rather than its initiation (Wendehenne et al., 2004). This may be due to the relative insensitivity of the fluorescent dye, as our data (Fig. 6) and those of others (Delledonne et al., 1998; Clarke et al., 2000) suggested that ·NO plays a role in the elicitation of cell death. We also observed ·NO production, although relatively delayed and at slower rates than during the HR when challenging with virulent bacteria. Such data were surprising given that both Delledonne et al. (1998) and Clarke et al. (2000) failed to observe any significant ·NO generation with virulent bacteria. Again, this may be due to the relative insensitivity of the assay methods used, which, in these cases, is based on reduced hemoglobin, compared to LPAD. Significantly, the more sensitive RIMS/MIMS approach detected elevated ·NO production in soybean cultures challenged with virulent *P. s.* pv *glycinea* (Conrath et al., 2004). In mammalian systems, low doses of ·NO can elicit or suppress apoptosis (Beligni and Lamattina, 1999) so that the low-level production of ·NO during compatible interactions could be important in pathogen virulence. When examining the effects of coinfiltration of *P. s.* pv *tabaci* with the ·NO scavenger CPTIO, in particular, we did not observe a decreased virulence, as might be the case if ·NO was acting as an anti-HR factor. Instead, greater *P. s.* pv *tabaci* virulence was observed, which was consistent with ·NO-mediating host defense mechanisms during compatible interactions.

To conclude, our data show that LPAD represents a highly sensitive and reproducible method for assessing ·NO production in planta. Using this increased sensitivity, we have demonstrated a rapid production of ·NO during a HR in tobacco, consistent with a role in the elicitation of cell death, as well as a novel action in suppressing disease development.

MATERIALS AND METHODS

Plant Growth and Chemicals

Tobacco (*Nicotiana tabacum*) cv Samsun NN was germinated in Levingtons universal compost (Levingtons Horticulture, Suffolk, UK) and transferred to John Innes No. 2 after 2 weeks. Tobacco plants were injected with bacterial suspensions or chemicals at 5 to 6 weeks following germination. All plants were grown at 22°C under a 16-h photoperiod. No fertilizer was added to the plants. ·NO donors, ·NO scavengers, and mammalian NOS inhibitors were purchased from Molecular Probes, Europe (Leiden, The Netherlands) or Calbiochem (CN BioSciences, Nottingham, UK).

Bacterial Strains and Inoculation Techniques and Estimation of Bacterial Populations

P. s. pv *phaseolicola* Race 6 strain 1,486 and *P. s.* pv *tabaci* strain 110,034 were used throughout. The culture and inoculation procedures used with these bacterial pathogens are described by Mur et al. (2000). Chemicals were injected or coinoculated with bacterial cultures into tobacco leaves using a 1-mL syringe with a 27-G needle (Terumo, Leuven, Belgium). Pathogens were grown at 28°C in nutrient agar (Oxoid Limited, Basingstoke, UK). The culture was washed twice with sterile, distilled water and finally diluted to either 10^8 (where changes in bacterial numbers over time were determined) or 10^6 (where ·NO levels were subsequently assessed) colony-forming units (cfu mL^{-1}) based on spectrophotometric readings (Mur et al., 2000). Estimations of bacterial populations were carried out as described by Mur et al. (2000). When scoring for *P. s.* pv *tabaci* disease symptom development, approximately 1-cm-diameter patches of leaf lamina were inoculated with bacteria using a 1-mL syringe without a needle.

When ·NO levels were measured or bacterial populations estimated, the entire leaf lamina was inoculated with culture and, as required, the chemical under assay, using a 5-mL syringae (Iwaki; Asahi Techno Glass, Tokyo) with a 2.5-G 5/8 needle (Microlance; Becton-Dickinson). All data were analyzed by *t* test, ANOVA, or χ^2, as appropriate, using MiniTab, version 13.

Estimations of Cell Death by Electrolyte Leakage

Changes in the conductivity of the solution bathing 1-cm-diameter leaf explants were determined as stated by Mur et al. (2000).

LPAD of Trace Gases

Traces of ·NO were measured down to approximately 1 ppbv (1:10^9)/approximately 20 pmol levels using a carbon monoxide (CO) laser-based photoacoustic detector (Fig. 2A). The evolved gases were detected via their absorption of rapidly chopped infrared light, which generated pressure variations, resulting in acoustic energy detected by a miniature microphone (Woltering et al., 1988; Bijnen et al., 1996). The intensity of the sound is proportional to the concentration of absorbing trace gas molecules. Trace gases emitted by the plants in the sampling cell were transported by a gas flow to the photoacoustic detection cell situated within the laser cavity. The source of the infrared light was a CO laser that was line tunable over a large frequency range in the infrared wavelength region (200 laser lines between 5.0- and 7.7-μm wavelength; Persijn et al., 2000). From a spectroscopic point of view, the properties of ·NO are well known. A high resolution of the fundamental band transition of ·NO covers a wavelength range between 5.1 and 5.6 μm (Spencer et al., 1994). The spectral coincidences between ·NO and the CO laser have been demonstrated by Garside et al. (1977) and List et al. (1979). Employing a CO laser-based photoacoustic detector, Bernegger and Sigrist (1990) measured the ·NO concentration in car exhaust. Since there is a mixture of trace gases in the detection cell and each gas has different absorption strength on every laser line, the mixed absorption strength pattern was unraveled using a multicomponent matrix calculation algorithm (Meyer and Sigrist, 1990).

A measurement was performed by flushing the carrier gas through the sampling cuvette, the cooling trap (at −80°C), and the photoacoustic cell. Three cuvettes were measured sequentially. One cuvette contained the infected tobacco leaf, the second cuvette a mock-infected (water-injected) tobacco leaf as control, and a third (empty) cuvette for measuring and subtracting the background signal. The residence period for the trace gases to flow from the sampling cuvette to the detection cell was approximately 60 s. The first data points were collected after 2.5 min.

ACKNOWLEDGMENTS

We thank Dr. Uwe Conrath (Aachen, Germany) for reading this manuscript and making valuable suggestions. Thanks also to Gerard van der Weerden and Walter Hendrickx (Nijmegen, The Netherlands), and Tom Thomas (University of Wales, Aberystwyth, UK) for growing and maintaining the tobacco plants. The *P. syringae* strains were a kind gift from Prof. John Mansfield (Wye College, Imperial College, UK). We appreciate the help provided by Drs. Paul Kenton and Andrew Clarke (University of Wales, Aberystwyth, UK) with ideas and manuscript preparation. The pathogen work was done under UK license PHF 123A/3624.

Received October 29, 2004; revised March 5, 2005; accepted March 23, 2005; published July 11, 2005.

LITERATURE CITED

Archer S (1993) Measurement of nitric oxide in biological models. FASEB J **7:** 349–360

Beligni MV, Lamattina L (1999) Is nitric oxide toxic or protective? Trends Plant Sci **4:** 299–300

Beligni MV, Lamattina L (2001) Nitric oxide: a non-traditional regulator of plant growth. Trends Plant Sci **6:** 508–509

Bernegger S, Sigrist MW (1990) CO-laser photoacoustic spectroscopy of gases and vapours for trace gas analysis. Infrared Phys **30:** 375–429

Bethke PC, Gubler F, Jacobsen JV, Jones RL (2004) Dormancy of Arabidopsis seeds and barley grains can be broken by nitric oxide. Planta **219:** 847–855

Bijnen FGC, Reuss J, Harren FJM (1996) Geometrical optimization of a longitudinal resonant photoacoustic cell for sensitive and fast trace gas detection. Rev Sci Instrum **67:** 2914–2923

Boamfa EI, Ram PC, Jackson MB, Reuss J, Harren FJM (2003) Dynamic aspects of alcoholic fermentation of rice seedlings in response to anaerobiosis and to complete submergence: relationship to submergence tolerance. Ann Bot (Lond) **91:** 279–290

Brookes PS, Bolanos JP, Heales SJR (1999) The assumption that nitric oxide inhibits mitochondrial ATP synthesis is correct. FEBS Lett **446:** 261–263

Brookes PS, Salinas EP, Darley-Usmar K, Eiserich JP, Freeman BA, Darley-Usmar VM, Anderson PG (2000) Concentration-dependent effects of nitric oxide on mitochondrial permeability transition and cytochrome c release. J Biol Chem **275:** 20474–20479

Brune B, von Knethen A, Sandau KB (1999) Nitric oxide (NO): an effector of apoptosis. Cell Death Differ **6:** 969–975

Chamnongpol SH, Willekens H, VanMontagu M, Inze D, Van Camp W (1998) Defence activation and enhanced pathogen tolerance induced by H_2O_2 in transgenic tobacco. Proc Natl Acad Sci USA **95:** 5818–5823

Clarke A, Desikan R, Hurst RD, Hancock JT, Neill SJ (2000) NO way back: nitric oxide and programmed cell death in *Arabidopsis thaliana* suspension cultures. Plant J **24:** 667–677

Collmer A, Badel JL, Charkowski AO, Deng WL, Fouts DE, Ramos AR, Rehm AH, Anderson DM, Schneewind O, van Dijk K, et al (2000) *Pseudomonas syringae* Hrp type III secretion system and effector proteins. Proc Natl Acad Sci USA **97:** 8770–8777

Conrath U, Amoroso G, Kohle H, Sultemeyer DF (2004) Non-invasive online detection of nitric oxide from plants and some other organisms by mass spectrometry. Plant J **38:** 1015–1022

Cristescu SM, de Martinis D, te Lintel Hekkert S, Parker DH, Harren FJM (2002) Ethylene production by *Botrytis cinerea* in vitro and in tomato fruit. Appl Environ Microbiol **68:** 5342–5350

Delledonne M, Xia Y, Dixon RA, Lamb C (1998) Nitric oxide functions as a signal in plant disease resistance. Nature **394:** 585–588

Delledonne M, Zeier J, Marocco A, Lamb C (2001) Signal interactions between nitric oxide and reactive oxygen intermediates in the plant hypersensitive disease resistance response. Proc Natl Acad Sci USA **98:** 13454–13459

de Pinto MC, Tommasi F, De Gara L (2002) Changes in the antioxidant systems as part of the signaling pathway responsible for the programmed cell death activated by nitric oxide and reactive oxygen species in tobacco Bright-Yellow 2 cells. Plant Physiol **130:** 698–708

Desikan R, Griffiths R, Hancock J, Neill S (2002) A new role for an old enzyme: nitrate reductase-mediated nitric oxide generation is required for abscisic acid-induced stomatal closure in Arabidopsis thaliana. Proc Natl Acad Sci USA **10:** 16314–16318

Dordas C, Hasinoff BB, Igamberdiev AU, Manac'h N, Rivoal J, Hill RD (2003) Expression of a stress-induced hemoglobin affects NO levels produced by alfalfa root cultures under hypoxic stress. Plant J **35:** 763–770

Dürner J, Wendehenne D, Klessig DF (1998) Defense gene induction in tobacco by nitric oxide, cyclic GMP, and cyclic ADP-ribose. Proc Natl Acad Sci USA **95:** 10328–10333

Fath A, Bethke PC, Jones RL (2001) Enzymes that scavenge reactive oxygen species are down-regulated prior to gibberellic acid-induced programmed cell death in barley aleurone. Plant Physiol **126:** 156–166

Foissner ID, Wendehenne D, Langebartels C, Dürner J (2000) In vivo imaging of an elicitor-induced nitric oxide burst in tobacco. Plant J **23:** 817–824

García-Mata C, Lamattina L (2003) Nitric oxide induces stomatal closure and enhances the adaptive plant responses against drought stress. Plant Physiol **126:** 1196–1204

Garside BK, Balik EA, Elsherbiny M, Shewchun J (1977) Resonance absorption measurement of NO with a line tuneable CO laser: spectroscopic data for pollution monitoring. Appl Opt **16:** 398–402

Groves JT, Wang CC (2000) Nitric oxide synthase: models and mechanisms. Curr Opin Chem Biol **4:** 687–695

Guo F-Q, Okamoto M, Crawford NM (2003) Identification of a plant nitric oxide synthase gene involved in hormonal signaling. Science **302:** 100–103

Harren FJM, Cotti G, Oomens J, te Lintel Hekkert S (2000) Photoacoustic spectroscopy in trace gas monitoring. *In* RA Meyers, ed, Encyclopedia of Analytical Chemistry. John Wiley, Chichester, UK, pp 2203–2226

Hughes MN (1999) Relationships between nitric oxide, nitroxyl ion, nitrosonium cation and peroxynitrite. Biochim Biophys Acta **1411:** 263–272

Kaiser WM, Weiner H, Kandlbinder A, Tsai CB, Rockel P, Sonoda M, Planchet E (2002) Modulation of nitrate reductase: some new insights, an unusual case and a potentially important side reaction. J Exp Bot **53:** 875–882

Kenton P, Mur LAJ, Atzorn R, Wasternack C, Draper J (1999) (−)-Jasmonic acid accumulation in tobacco hypersensitive response lesions. Mol Plant Microbe Interact **12:** 74–78

Kojima H, Nakatsubo N, Kikuchi K, Kawahara S, Kirino Y, Nagoshi H,

Hirata Y, Nagano T (1998) Detection and imaging of nitric oxide with novel fluorescent indicators: diaminofluoresceins. Anal Chem **70:** 2446–2453

Leone AM, Rhodes P, Furst V, Moncada S (1995) Techniques for the measurement of nitric oxide. *In* DA Kendal, SJ Hill, eds, Methods in Molecular Biology, Vol 41: Signal Transduction Protocols. Humana Press, Totowa, NJ

Leprince OFJ, Harren F, Buitink J, Alberda M, Hoekstra FA (2000) Metabolic dysfunction and unabated respiration precede the loss of membrane integrity during dehydration of germinating radicles. Plant Physiol **122:** 597–608

Leshem YY, Pinchasov Y (2000) Non-invasive photoacoustic spectroscopic determination of relative endogenous nitric oxide and ethylene content stoichiometry during the ripening of strawberries *Fragaria anannasa* (Duch.) and avocados *Persea americana* (Mill.). J Exp Bot **51:** 1471–1473

Leshem YY, Wills RBH, Ku VVV (1998) Evidence for the function of the free radical gas—nitric oxide (NO)—as an endogenous maturation and senescence regulating factor in higher plants. Plant Physiol Biochem **36:** 825–833

Levine AR, Tenhaken R, Dixon R, Lamb C (1994) H_2O_2 from the oxidative burst orchestrates the plant hypersensitive disease resistance response. Cell **79:** 583–593

List U, Hermann W, Urban W, Fink EH (1979) Spectral coincidences between CO-laser and nitric oxide, a reinvestigation. Appl Physics **19:** 427–429

Malinski T, Bailey F, Zhang ZG, Chopp M (1993) Nitric oxide measured by a porphyrinic microsensor in rat brain after transient middle cerebral artery occlusion. J Cereb Blood Flow Metab **13:** 355–358

Meyer PL, Sigrist MW (1990) Atmospheric pollution monitoring using CO_2 laser photoacoustic spectroscopy and other techniques. Rev Sci Instrum **61:** 1779–1807

Morot-Gaudry-Talarmain Y, Rockel P, Moureaux T, Quillere I, Leydecker MT, Kaiser WM, Morot-Gaudry JF (2002) Nitrite accumulation and nitric oxide emission in relation to cellular signaling in nitrite reductase antisense tobacco. Planta **215:** 708–715

Mur LAJ, Brown IR, Darby RM, Bestwick CS, Bi YM, Mansfield JW, Draper J (2000) A loss of resistance to avirulent bacterial pathogens in tobacco is associated with the attenuation of a salicylic acid-potentiated oxidative burst. Plant J **23:** 609–621

Mur LAJ, Santosa IE, Laarhoven L-JJ, Holton NJ, Harren F, Smith AR (2003) A new partner in the *danse macabre*: the role of nitric oxide in the hypersensitive response. Bul J Plant Physiol (Special issue) 110-123

Murphy ME, Noack E (1994) Nitric oxide assay using haemoglobin method. Methods Enzymol **233:** 240–250

Mysore KS, Ryu CM (2004) Nonhost resistance: how much do we know? Trends Plant Sci **9:** 97–104

Pedroso MC, Magalhaes JR, Durzan D (2000) A nitric oxide burst precedes apoptosis in angiosperm and gymnosperm callus cells and foliar tissues. J Exp Bot **51:** 1027–1036

Persijn ST, Veltman RH, Oomens J, Harren FJM, Parker DH (2000) CO laser absorption coefficients of biological relevance: H_2O, CO_2, ethanol acetaldehyde and ethylene. Appl Spectrosc **54:** 62–71

Orozco-Cardenas ML, Ryan CA (2002) Nitric oxide negatively modulates wound signaling in tomato plants. Plant Physiol **130:** 487–493

Rockel P, Strube F, Rockel A, Wildt J, Kaiser WM (2002) Regulation of nitric oxide (NO) production by plant nitrate reductase *in vivo* and *in vitro*. J Exp Bot **53:** 103–110

Rohmer L, Kjemtrup S, Marchesini P, Dangl JL (2003) Nucleotide sequence, functional characterization and evolution of pFKN, a virulence plasmid in *Pseudomonas syringae* pathovar *maculicola*. Mol Microbiol **47:** 1545–1562

Sakihama Y, Nakamura S, Yamasaki H (2002) Nitric oxide production mediated by nitrate reductase in the green alga *Chlamydomonas reinhardtii*: an alternative NO production pathway in photosynthetic organisms. Plant Cell Physiol **43:** 290–297

Saviani EE, Orsi CH, Oliveira JF, Pinto-Maglio CA, Salgado I (2002) Participation of the mitochondrial permeability transition pore in nitric oxide-induced plant cell death. FEBS Lett **510:** 136–140

Shibuki K (1990) An electrochemical microprobe for detecting nitric oxide release in brain tissue. Neurosci Res **9:** 69–76

Spencer MN, Chackerian C Jr, Giver L (1994) The nitric oxide fundamental band: frequency and shape parameter for ro-vibrational lines. J Mol Spectrosc **165:** 506–524

Tada Y, Mori T, Shinogi T, Yao N, Takahashi S, Betsuyaku S, Sakamoto M, Park P, Nakayashiki H, Tosa Y, et al (2004) Nitric oxide and reactive oxygen species do not elicit hypersensitive cell death but induce apoptosis in the adjacent cells during the defense response of oat. Mol Plant Microbe Interact **7:** 245–253

van den Bussche F, Smalle J, Le J, Saibo NJ, de Paepe A, Chaerle L, Tietz O, Smets R, Laarhoven LJJ, Harren FJM, et al (2003) The Arabidopsis mutant *alh 1* illustrates a cross talk between ethylene and auxin. Plant Physiol **131:** 1228–1238

Wendehenne D, Durner J, Klessig DF (2004) Nitric oxide: a new player in plant signaling and defence responses. Curr Opin Plant Biol **7:** 449–455

Wendehenne D, Pugin A, Klessig DF, Dürner J (2001) Nitric oxide: comparative synthesis and signaling in animal and plant cells. Trends Plant Sci **6:** 177–183

Woltering EJ, Harren F, Boerrigter HAM (1988) Use of a laser driven photoacoustic detection system for measurements of ethylene production in Cymbidium flowers. Plant Physiol **88:** 506–510

Zeier J, Delledonne M, Mishina T, Severi E, Sonoda M, Lamb C (2004) Genetic elucidation of nitric oxide signaling in incompatible plant-pathogen interactions. Plant Physiol **136:** 2875–2886

Zhang C, Czymmek KJ, Shapiro AD (2003) Nitric oxide does not trigger early programmed cell death events but may contribute to cell-to-cell signaling governing progression of the Arabidopsis hypersensitive response. Mol Plant Microbe Interact **16:** 962–972

Zweier JL, Samouilov A, Kuppusamy P (1999) Non-enzymatic nitric oxide synthesis in biological systems. Biochim Biophys Acta **1411:** 250–262